ACS APPLIED MATERIALS & INTERFACES

Research Article

www.acsami.org

Water-Stable, Adaptive, and Electroactive Supramolecular Ionic Material and Its Application in Biosensing

Li Zhang, Hetong Qi, Jie Hao, Lifen Yang, Ping Yu,* and Lanqun Mao*

Beijing National Laboratory for Molecular Sciences, Key Laboratory of Analytical Chemistry for Living Biosystems, Institute of Chemistry, the Chinese Academy of Sciences, Beijing 100190, P. R. China

Supporting Information

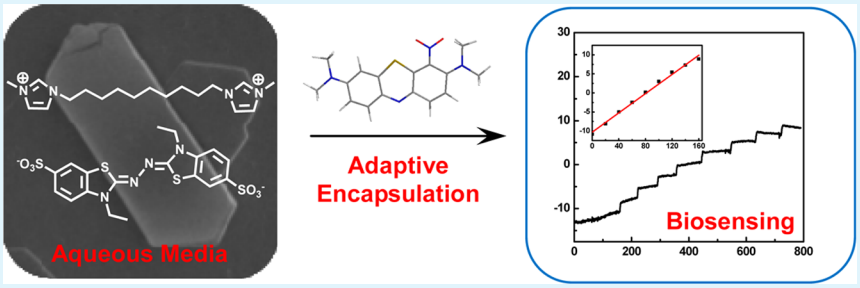

ABSTRACT: Developing water-stable and adaptive supramolecular materials is of great importance in various research fields. Here, we demonstrate a new kind of water-stable, adaptive, and electroactive supramolecular ionic materials (SIM) that is formed from the aqueous solutions of imidazolium-based dication and dianionic dye (i.e., 2,2′-azino-bis(3-ethylbenzothiazoline-6-sulfonic acid), ABTS) through ionic self-assembly. The formed SIM not only shows good thermostability and unique optical and electrochemical properties that are raised from precursors of the SIM, but also exhibits good water-stability, salt-stability, and adaptive encapsulation properties toward some heterocyclic cationic dye molecules. UV−vis and FT-IR results demonstrate that this encapsulation property is essentially based on the electrostatic interactions between the guest dye molecules and ABTS in the SIM. The application of the SIM prepared here is illustrated by the development of a new electrochemical sensor for NADH sensing at a low potential. This study not only opens a new avenue to the preparation of the supramolecular materials, but also provides a versatile platform for electrochemical (bio)sensing.

KEYWORDS: *supramolecular ionic materials, water-stable, adaptive encapsulation, electrochemistry, biosensor*

INTRODUCTION

Over the past two decades, functional supramolecular materials prepared with noncovalent interactions have attracted enormous attention[1−3] because of their unique applications in electronics,[4−6] photonics,[7,8] light-energy conversion,[9−11] biosensing,[12,13] and catalysis.[14,15] Recently, supramolecular materials with water-stability and adaptive encapsulation properties have become particularly attractive especially in biosensor development since most biological processes take place in aqueous environments and biological molecules such as proteins and enzymes are generally active in water. Moreover, the ability to encapsulate functional molecules in supramolecular networks enables the materials to hold great promise in tailoring and improving their functions for target-oriented applications.[16] So far, several kinds of water-stable and adaptive materials have been developed, mainly based on metal-coordination interactions.[17−19] As a result, it is imperative to explore other kinds of noncovalent interactions for the development of water-stable and adaptive materials with excellent properties.

Ionic interaction between oppositely charged species represents one of the strongest noncovalent interactions and has been widely used in self-assembly, typically as electrostatic self-assembly in solid state[20] and ionic self-assembly in solution.[21−23] All this work suggests that Coulombic interaction could be used as the noncovalent interaction to form supramolecular materials by self-assembly. While wide availability of charged species and the simplicity of their synthesis allow the ionic interactions to be used in synthesis of various functional materials, it remains a great challenge to utilize this kind of interaction to develop functional supramolecular materials with water stability and adaptive encapsulation property. This is because, on one hand, most of the charged species could easily dissolve in water because of the high dielectric constant of water (ε = 78.5, at 25 °C) and thus the electrostatic interactions become significantly weakened in water. On the other hand, the large lattice energy in ionic compounds essentially limits their encapsulation property. Very recently, this interaction was utilized to create supramolecular ionic networks and supramolecular polymers[24,25] by using multiple electrostatic bonds. This implies that ionic interaction could potentially provide the possibility to form water-stable

Received: February 25, 2014
Accepted: April 2, 2014
Published: April 2, 2014

dx.doi.org/10.1021/am5011628 | ACS Appl. Mater. Interfaces 2014, 6, 5988−5995

and adaptive supramolecular materials by rationally designing the structure of the building blocks. However, such potential has not been explored so far.

We found herein a new kind of supramolecular ionic material (SIM) that could be readily formed in water by ionic self-assembly from imidazolium-based dication, i.e., 1,10-bis(3-methylimidazolium-1-yl) decane ($C_{10}(mim)_2$), and dianion, i.e., 2,2′-azino-bis(3-ethylbenzothiazoline-6-sulfonic acid) (ABTS) (Figure 1). The geminal imidazolium dication was selected as the building block for preparation of supramolecular ionic materials since symmetric dications have recently been of great interest in a variety of applications, and the two positive charges in the dication are favorable for formation of the supramolecular ionic network.[24,26] Moreover, the imidazolium dication displays unique optical properties. The formed SIM shows good water-stability, good salt-stability, and excellent electrochemical/optical properties. Moreover, the SIM exhibits an adaptive encapsulation property toward some heterocyclic cationic dye molecules during the self-assembly process. This property was considered to originate from the electrostatic interaction between dye molecule and ABTS. Based on this, the electrochemical sensor for NADH was constructed by using the present SIM. We believe that the concept demonstrated here could provide a new approach to development of functional materials that have excellent properties distinct from the materials formed with metal−ligand interactions, and are thus particularly useful in many research fields, especially biosensing and drug delivery.

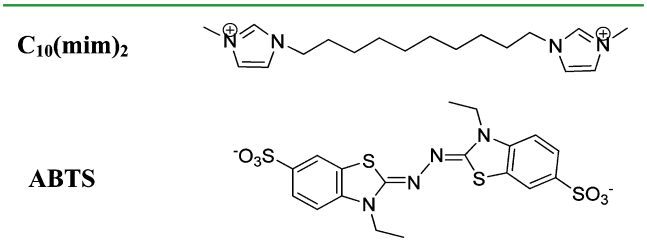

Figure 1. Chemical structures of the dication and dianion.

EXPERIMENTAL SECTION

Materials. 2, 2′-Azino-bis (3-ethylbenzothiazoline-6-sulfonic acid) (ABTS) diammonium salt, acridine orange (AO), rhodamine 6G (Rh6G), and dihydronicotinamide adenine dinucleotide (NADH) were purchased from Sigma-Aldrich and used as supplied. Laccase (E.C. 1.10.3.2, from Trametes versicolor) was also purchased from Sigma-Aldrich and purified with a method described in our earlier work.[27] Bovine serum albumin (BSA) was obtained from Proliant (USA). Rhodamine B (RhB), and safranine T (ST), 1-methylimidazole, and 1,10-dibromodecane were obtained from Aladdin. Methylene green (MG) and methylene blue (MB) were purchased from Beijing Chemical Co. (Beijing, China). All aqueous solutions were prepared with Milli-Q water.

Apparatus. The morphology and size of the materials were characterized by field emission scanning electron microscopy (FE-SEM, Hitachi S-4800, and S-4300) at an accelerating voltage of 15 kV. Thermal gravimetric analysis (TGA) was performed on a Netzsch STA 409 PC/PG thermal analyzer. The samples were deposited in an alumina crucible and heated in a continuous flow of nitrogen gas with a ramp rate of 10 °C/min from room temperature to 1000 °C. Powder X-ray diffraction (PXRD) patterns were recorded at room temperature on a Rigaku X-ray Diffractometer (D/max-2500) with an X-ray source of Cu Kα (λ = 1.54056 Å) at 40 kV and 200 mA. FT-IR spectra (KBr pellet) were collected on a Tensor-27 FTIR spectrometer (Bruker). X-ray photoelectron spectroscopy (XPS) data were obtained with an ESCALab220i-XL electron spectrometer from VG Scientific using 300 W Al Kα radiation. The base pressure was about 3×10^{-9} mbar. Elemental analysis was performed using a flash EA 1112 NC analyzer from Thermo Scientific. UV−vis diffuse reflection spectroscopy (UV−vis DRS) for solid samples and UV−vis spectra for liquid samples were recorded by a TU-1901 spectrophotometer (Beijing Purkinje General Instrument Co. Ltd., China). Confocal laser scanning microscopy (CLSM) images were performed on an Olympus FV1000-IX81 CLSM

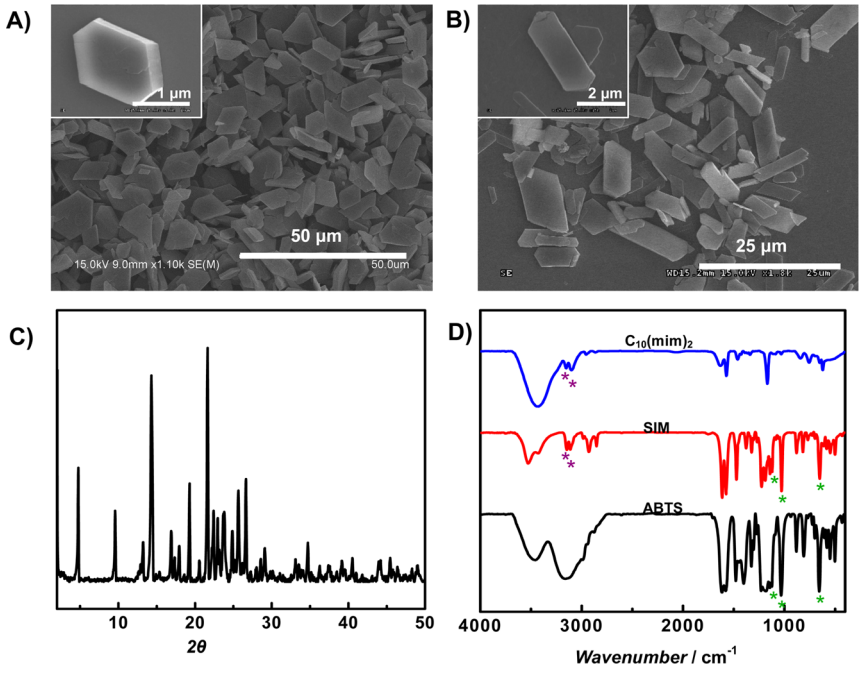

Figure 2. SEM images of SIM self-assembled from equimolar aqueous solutions of $C_{10}(mim)_2$ and ABTS dianion at different concentrations of 20 mM (A) and 500 μM (B). (C) Powder X-ray diffraction (PXRD) pattern of the as-prepared SIM. (D) FT-IR spectra of $C_{10}(mim)_2$ (bromide salt, blue curve), SIM (red curve), and ABTS (ammonium salt, black curve).

dx.doi.org/10.1021/am5011628 | ACS Appl. Mater. Interfaces 2014, 6, 5988−5995

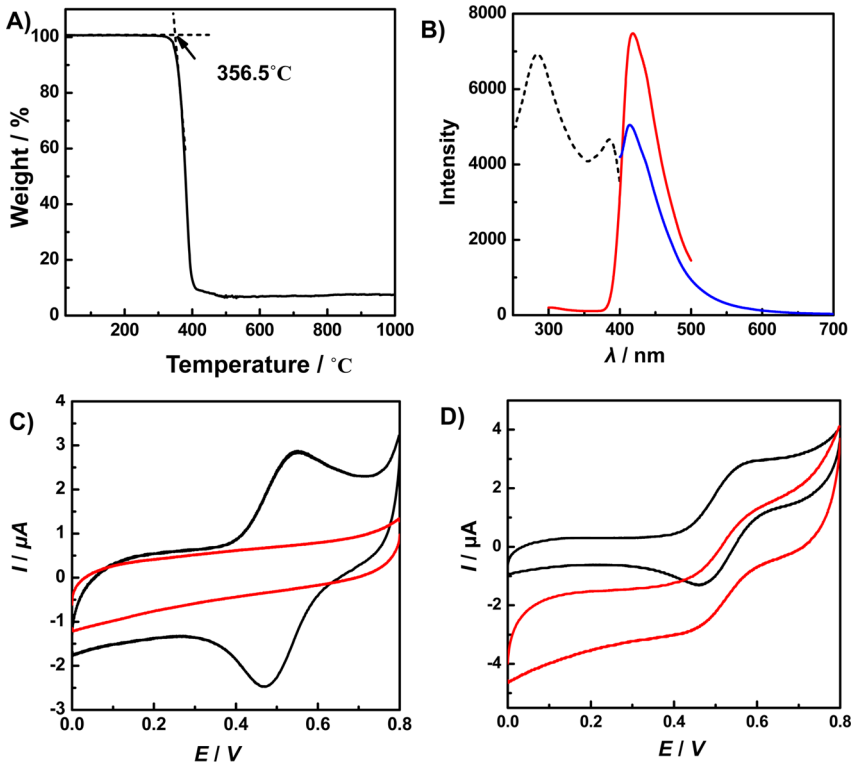

Figure 3. (A) Thermal gravimetric analysis (TGA) curve of the SIM. (B) Solid fluorescence spectra of the SIM: the excitation spectrum with λ_{em} = 418 nm (dashed black curve) and the emission spectra with λ_{ex} = 284 nm (red solid curve) and λ_{ex} = 385 nm (blue solid curve). (C) Cyclic voltammograms (CVs) obtained at bare (red curve) and SIM-modified (black curve) glassy carbon (GC) electrode in phosphate buffer (0.10 M, pH 6.0) at a scan rate of 100 mV s^{-1}. (D) CVs obtained at the SIM/laccase-modified GC electrode in phosphate buffer (0.10 M, pH 6.0) saturated with nitrogen (black curve) and oxygen (red curve). Scan rate, 100 mV s^{-1}.

and a Leica TCS SP confocal system (Leica, Germany). Fluorescence emission spectra were recorded by a Hitachi F-4600 fluorescence spectrophotometer.

Synthesis of Dication $C_{10}(mim)_2$.[26] Typically, 11.4 g (0.038 mol) of 1,10-dibromodecane was added dropwise into 6 mL (0.075 mol) of 1-methylimidazole in a round-bottom flask under constant stirring at room temperature, and the reaction was maintained for 5 h. The resulting mixture was dissolved in 50 mL of water and extracted with 25 mL of ethyl acetate three times. Water was removed using rotary evaporator (RE 52AA) and the remaining salt was dried in a vacuum drying oven (DZF 6020). ^{1}H-NMR (DMSO, 400 MHz): δ ppm 9.24 (s, 2H); 7.81 (t, 2H); 7.74 (t, 2H); 4.17 (t, 4H); 3.86 (s, 6H); 1.77 (t, 4H); 1.26 (s, 12H). The hydroxide-exchanged form of $C_{10}(mim)_2$ was obtained through anion exchange with bromide salts of $C_{10}(mim)_2$ using 717 ion-exchange resin.

Synthesis of SIM. The synthesis of SIM from $C_{10}(mim)_2$ dication and ABTS dianion in water was conducted by mixing an aqueous solution of a hydroxide-exchanged form of $C_{10}(mim)_2$ with equimolar ABTS (1 mM) to produce white precipitate. The precipitate was washed with water several times and collected by centrifugation.

Number of Dyes Encapsulated into SIM. To determine the number of dyes encapsulated into the SIM, 0.5 mg of each dye-encapsulated SIM was dissolved into 5 mL of ethanol/water mixture (v/v, 50%), and the absorbance at maximal absorption for each kind of dye was recorded. According to the Lambert−Beer law, we estimated the content of dye by comparing the above-recorded absorbance to that of pure dye in 50% ethanol/water mixture (5 μg/mL).

Electrochemistry. Electrochemical measurements were carried out with a computer-controlled electrochemical analyzer (CHI 842D, Shanghai, China) in a two-compartment and three-electrode cell. Glassy carbon electrodes (GC, 3 mm diameter) were used as substrate electrode to investigate the electrochemical properties and biosensing applications of the SIM. For the electrochemical studies, pure SIM (i.e., without MG encapsulation) or MG-encapsulated SIM was confined onto GC electrodes by dip-coating 3 μL of pure or MG-encapsulated SIM dispersion (1 mg/mL) onto GC electrodes, and the electrodes were then air-dried. The SIM-based laccase electrodes were prepared by dip-coating 4 μL of mixture consisting of laccase (2 μL, purified), BSA (1 μL, 1%), and gluteraldehyde (1 μL, 1%) onto the SIM-modified electrodes. For all electrochemical measurements, the GC electrodes were used as working electrode, a platinum spiral wire as counter electrode, and a Ag/AgCl electrode (KCl-saturated) as reference electrode. A 0.10 M phosphate buffer was used as electrolyte. Electrochemical measurements were conducted at room temperature.

RESULTS AND DISCUSSION

SIM Prepared by Self-Assembly from $C_{10}(mim)_2$ and ABTS in Water. The SIM was prepared from $C_{10}(mim)_2$ and ABTS in water through self-assembly and formation of hexagonal microstructure was characterized with scanning electron microscopy (SEM) (Figure 2A and B). The size of the hexagonal structure ranges from several to tens of micrometers with the thickness varying from hundreds of nanometers to several micrometers, suggesting a nearly two-dimensional (2D) microstructure of the ionic material. This regular hexagonal structure could be tuned by changing the concentration of the precursor: when a low concentration of the precursor was used, the material preferentially formed more regular 2D microstructures, as shown in Figure 2B. Moreover, this hexagonal microstructure of precipitates likely results from a preferred arrangement of the building blocks, which was confirmed by the powder X-ray diffraction (PXRD), in which the materials are highly crystalline (Figure 2C). The stoichiometry of materials determined by elemental analysis and X-ray photoelectron spectroscopy (XPS) was

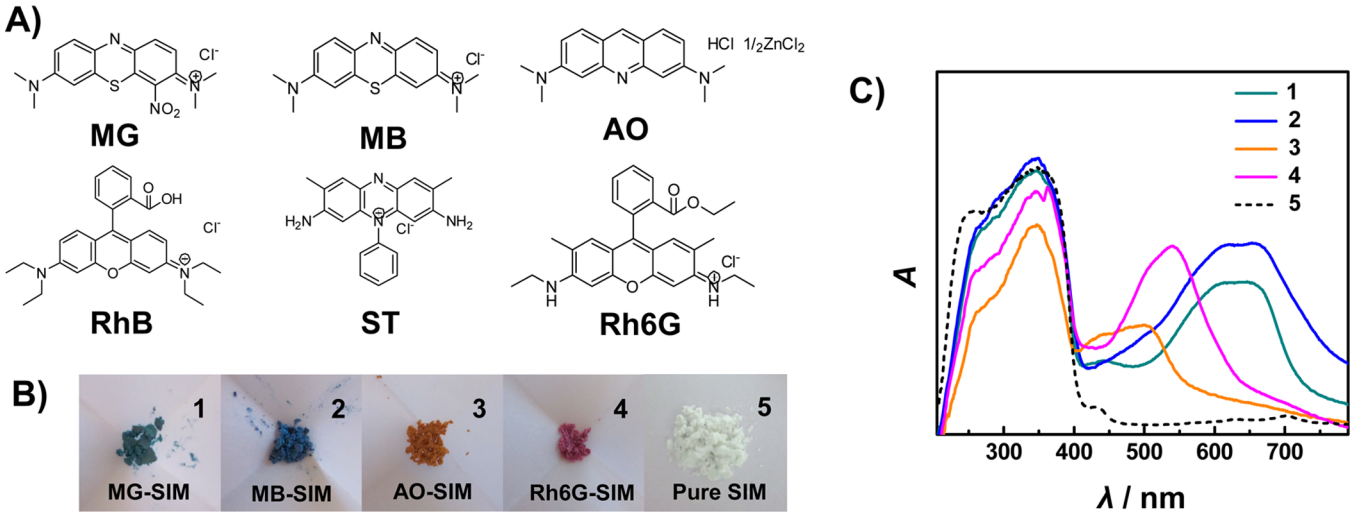

Figure 4. (A) Chemical structures of dyes under investigation. (B) Photographs and (C) UV−vis DRS spectra of the dye-encapsulated SIMs: (1) MG-encapsulated SIM, (2) MB-encapsulated SIM, (3) AO-encapsulated SIM, (4) Rh6G-encapsulated SIM, and (5) pure SIM (i.e., without dye encapsulation).

ABTS:$C_{10}(mim)_2$ = 1:1 (Table S1). This value demonstrates that the formation of hexagonal material is induced by electrostatic interaction between oppositely charged ions.[16] Moreover, after the formation of SIM, the characteristic peaks of sulfonate in ABTS molecules[28] shift from 1124, 1032, and 656 cm^{-1} to 1121, 1027, and 651 cm^{-1}, respectively, while the stretching frequency of C_2−H in imidazolium[29−31] shifts from 3100 and 3152 cm^{-1} to 3112 and 3145 cm^{-1}, respectively (Figure 2D). These shifts in FT-IR spectra also demonstrate that the oppositely charged ions could be self-assembled by strong electrostatic interaction in aqueous media.

Properties of the SIM. The as-prepared SIM shows intrinsic properties such as thermostability and good optical/electrochemical properties. The thermal behavior of the SIM was investigated by TGA. As shown in Figure 3A, the SIM starts to degrade at 356.5 °C, which is higher than for the bromide salt of $C_{10}(mim)_2$ (316.5 °C) and amino salt of ABTS (300.3 °C) (Figure S1), demonstrating that the formed SIM bears better thermostability than the precursors. The SIM synthesized in this study also shows good optical and electrochemical properties, which mainly originated from the precursors of the SIM. For example, a strong fluorescence emission was observed at 418 nm upon excitation at 284 and 385 nm. This emission was considered to arise from the imidazolium dications (Figure 3B).[32−35] Moreover, a pair of well-defined redox peaks at 0.51 V (vs Ag/AgCl) was observed at the SIM modified-electrode (Figure 3C). This potential was almost consistent with that of the ABTS precursor, demonstrating that the as-prepared SIM keeps the electrochemical properties of the ABTS precursor.[36] More importantly, the as-prepared SIM exhibits some distinct properties from the traditional ionic compounds. First, since the SIM was self-assembled from the aqueous media, it is difficult to dissolve into water and thus shows good water-stability. Second, the SIM exhibits strong salt-stability. Typically, when the SIM (0.8 mg) was dispersed into 500 mM KCl solution (1 mL), the precipitate was still clearly observed (Figure S2a). After being washed with water three times and collected by centrifugation, the regular hexagonal microstructures of the SIM were still kept (Figure S2b), demonstrating that as-formed SIM was quite stable in the aqueous solution of 500 mM KCl. This feature was remarkable since most ionic compounds are usually not very stable in a high salt solution.

The excellent properties of the SIM prepared here make it very promising for applications in many research fields such as some biorelated applications. For example, although ABTS itself has good electrochemical properties and is always expected to be used to construct the bioanodes for enzymatic biofuel cells, its good solubility in water essentially renders difficulties in the development of this kind of integrated biogenerator. In this context, the SIM with good water and salt stability could easily be immobilized onto an electrode surface to form an integrated bioanode after cross-linking of laccase. As shown in Figure 3D, upon cross-linking of laccase, the SIM-modified electrode exhibits good bioelectrocatalytic activity toward the reduction of oxygen. This property validates the as-prepared SIM for the development of advanced enzymatic biofuel cells.

Adaptive Encapsulation of Dyes in SIM. To demonstrate the adaptive encapsulation property of the SIM toward some water-soluble dyes during the self-assembly process, we selected six kinds of heterocyclic cationic dye molecules (i.e., methylene green (MG), methylene blue (MB), acridine orange (AO), rhodamine 6G (Rh6G), rhodamine B (RhB) and safranine T (ST)) (structural formula, see Figure 4A) as the guest molecules. With addition of the same concentration of each dye, adaptive encapsulation was observed for the dye molecules of MG, MB, AO, and Rh6G from both the color change of the precipitates (Figure 4B) and the absorption behavior in the visible region of the UV−vis DRS spectra (Figure 4C). We did not observe obvious encapsulation for RhB or ST (Figure S3). Moreover, UV−vis DRS spectra of dye-encapsulated SIMs show shifts in the absorption peaks compared with those of pure dyes (Figure S4), indicating that the dyes were not simply physically encapsulated into the SIM. Furthermore, SEM images and powder X-ray diffraction patterns reveal that both morphology and crystallization pattern of the SIM changed after dye encapsulation (Figures S5 and S6), probably due to interactions of the dyes and the precursors of SIM (i.e., ABTS or $C_{10}(mim)_2$), which were demonstrated below.

dx.doi.org/10.1021/am5011628 | ACS Appl. Mater. Interfaces 2014, 6, 5988−5995

Encapsulation of dyes into the SIM was also investigated by confocal laser scanning microscopy (CLSM) with Rh6G as a model dye. As displayed in Figure 5, the as-prepared pure SIM

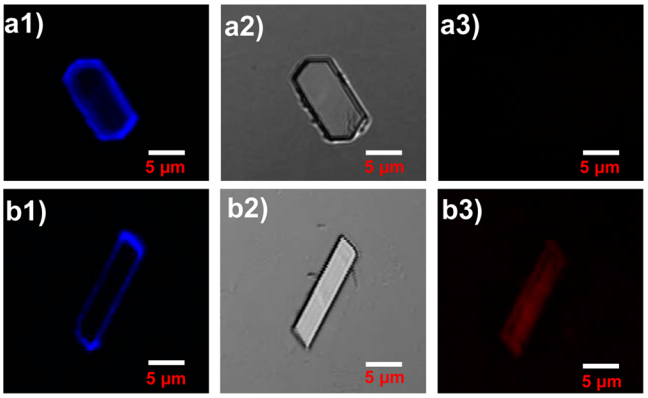

Figure 5. (a) Confocal fluorescence (a1 and a3) and bright-field (a2) images of pure SIM. λ_{ex} = 405 nm (a1) and λ_{ex} = 559 nm (a3). (b) Confocal fluorescence (b1 and b3) and bright-field (b2) images of Rh6G-encapsulated SIM. λ_{ex} = 405 nm (b1) and λ_{ex} = 559 nm (b3).

emits a strong blue fluorescence at λ_{ex} = 405 nm (a1), which originated from the emission of imidazolium-based dication (i.e., $C_{10}(mim)_2$). After Rh6G encapsulation, the as-formed material also exhibits a strong blue fluorescence at λ_{ex} = 405 nm (b1). By contrast, the Rh6G-encapsulated SIM emits red fluorescence at λ_{ex} = 559 nm (b3), while there was no emission for the pure SIM at λ_{ex} = 559 nm (a3). A similar phenomenon was observed for the AO-encapsulated SIM (Figure S7). All these results demonstrate that this kind of supramolecular material bears an adaptive encapsulation ability toward some heterocyclic dye molecules, which creates a new avenue to the formation of functional materials.

To investigate the mechanism for dye encapsulation, the interaction between dyes and pure ABTS or $C_{10}(mim)_2$ was studied with UV−vis and FT-IR. When ABTS was added into the aqueous solution of each kind of dye (i.e., MG, MB, AO, Rh6G, RhB, and ST), the UV−vis absorption of each dye shows an obvious red shift, while the addition of $C_{10}(mim)_2$ did not (Figure 6A,B). These results demonstrate that the encapsulation capability observed above mainly originated from the interaction between ABTS anion, rather than $C_{10}(mim)_2$ cation, and the dyes. As a support, we found that the dyes (i.e., RhB and ST) show a weaker interaction with ABTS, as compared with the other four kinds of dyes, and thus could not be encapsulated into the SIM (Figure 6A). The FT-IR spectra of pure dyes and the precipitates formed from high concentrations of ABTS and each of the four kinds of dyes also support our speculation. Typically, after formation of the precipitates with MB, the symmetric vibration bands of sulfonate in ABTS show a significant shift from 1124, 1032, and 656 cm^{-1} to 1121, 1028, and 650 cm^{-1}, respectively, while the N−CH_3 stretching and C=N^+ vibration bands of MB[37] show an obvious shift from 1178, 1141, and 1601 cm^{-1} to 1176, 1139, and 1600 cm^{-1}, respectively (Figure 6C). Similar phenomena were also observed for those of MG, Rh6G, and AO[38,39] (Figure S8a-c), suggesting that the encapsulation of dyes into the SIM was based on the interaction (mainly electrostatic interaction) between ABTS and the dyes. For RhB and ST, the existence of a carboxylate group in RhB and the substitute of a phenyl group in ST may weaken the electrostatic interaction with ABTS, resulting in failure in the encapsulation.

The numbers of the dye molecules encapsulated into the SIM were evaluated by dissolving the dye-encapsulated SIMs into a 50% water/ethanol mixture and measuring the UV−visible absorbance of the resulting mixtures. The numbers of dye molecules encapsulated into the 100 SIM molecules were calculated to be ca. 4 for MG, 10 for MB, 2 for AO, and 6 for Rh6G. These numbers were much higher than those in the dye inclusion crystal systems reported previously, in which the crystal systems were mainly constructed of inorganic salts or small organic molecules, and dyes included in the crystal have no interaction with the crystal matrix.[40,41] The larger numbers obtained in our SIMs could be presumably ascribed to the adaptive property of the SIMs for dye encapsulation. To the best of our knowledge, there is no report on the encapsulation property of the SIMs and this unique property endows the SIM prepared in this study with attractive applications such as biosensing, as demonstrated below.

Electrochemistry of MG-Encapsulated SIM and Its Application for NADH Sensing. The water and salt stability and the adaptive encapsulation property of the as-prepared SIMs enable their application in various fields, especially in (bio)sensing. Here, we used MG-encapsulated SIM as an example to illustrate the potential applications of the dye-encapsulated SIMs since MG possesses good electrochemical

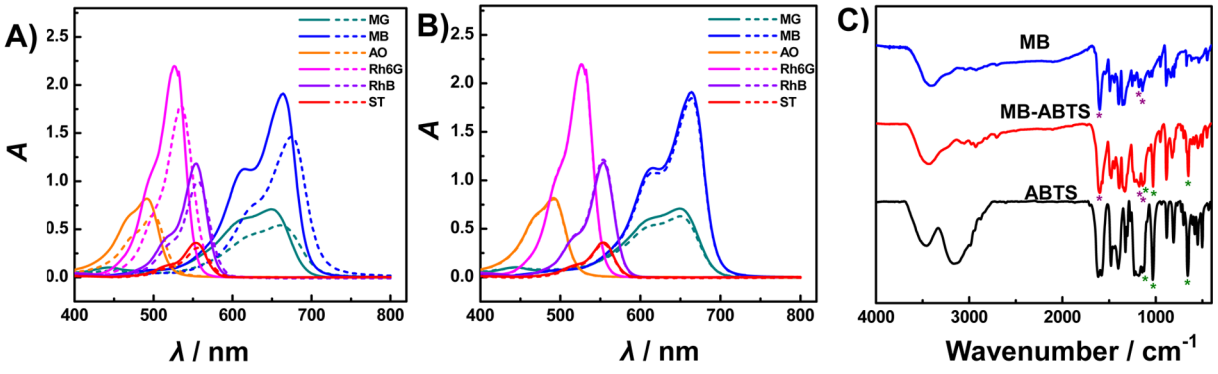

Figure 6. (A) UV−vis spectra of 25 μM aqueous solution of pure dyes (solid curves), and the mixture of 25 μM dye and 250 μM ABTS (dashed curves). (B) UV−vis spectra of 25 μM aqueous solution of pure dyes (solid curves), and the mixture of 25 μM dye and 250 μM $C_{10}(mim)_2$ (dashed curves). (C) FT-IR spectra of chlorine salts of MB (blue curve), precipitates formed by MB and ABTS (red curve), and pure ABTS (ammonium salt, black curve).

dx.doi.org/10.1021/am5011628 | ACS Appl. Mater. Interfaces 2014, 6, 5988−5995

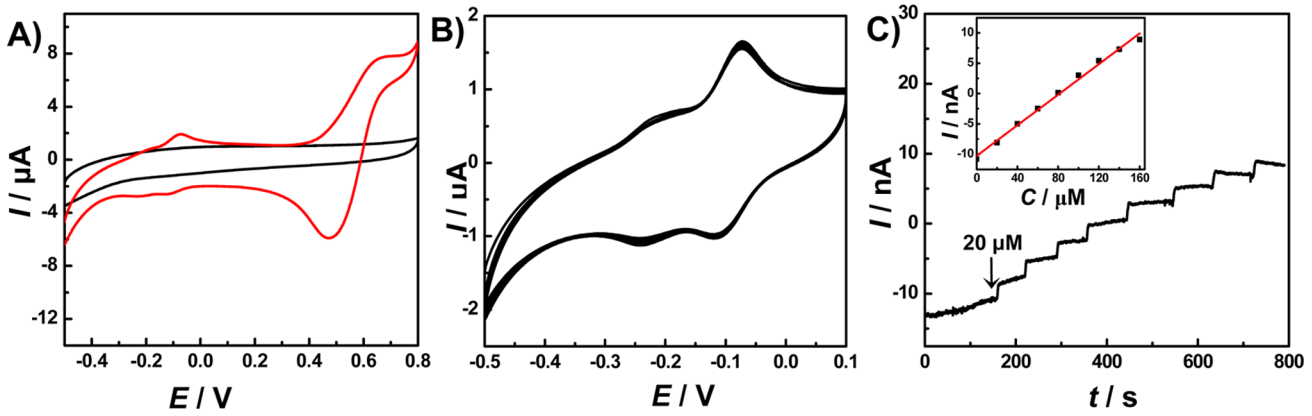

Figure 7. (A) Cyclic voltammograms (CVs) obtained at bare (black curve) and MG-encapsulated SIM-modified (red curve) GC electrode in nitrogen-saturated phosphate buffer (0.10 M, pH 7.0). Scan rate, 100 mV s^{-1}. (B) Consecutive CVs for 50 cycles obtained at the MG-encapsulated SIM-modified GC electrode in nitrogen-saturated phosphate buffer (0.10 M, pH 7.0). Scan rate, 100 mV s^{-1}. (C) Typical amperometric responses obtained at the MG-encapsulated SIM-modified GC electrode in nitrogen-saturated phosphate buffer (0.10 M, pH 7.0) toward successive addition of NADH into the buffer. Applied potential, −0.07 V. Inset: plot of current response versus NADH concentration.

properties and has been widely used for fundamental electrochemical studies and applications, such as biosensors and biofuel cells. As shown in Figure 7A, the as-formed MG-encapsulated SIM shows three pairs of well-defined redox peaks at ca. −0.21 V, −0.095 V, and +0.56 V. The peaks at −0.21 V and −0.095 V were ascribed to the redox process of the encapsulated MG in the SIM and the wave at +0.56 V was attributed to the electrochemical process of ABTS in the SIM. This result demonstrated that the encapsulated MG exhibits good electrochemical properties that were comparable to those of MG confined on carbon materials.[42] Moreover, the electrochemical behavior of the encapsulated MG shows very good stability. Figure 7B displays consecutive CVs obtained at the MG-encapsulated SIM-modified GC electrode in 0.10 M phosphate buffer (pH 7.0). The peak current did not show an obvious change upon consecutively cycling the electrode for 50 cycles, revealing good stability of MG-encapsulated SIM on the electrode. This property could originate from the good water and salt stability of the SIM, which is of great importance for the development of electrochemical (bio)sensors.

To further demonstrate the potential application of the as-prepared SIM in (bio)sensor development, an electrochemical sensor for NADH was constructed. Electrocatalytic oxidation and sensing of NADH have been receiving great attention from the viewpoint of developing dehydrogenase-based biodevices such as biosensors and biofuel cells, since NADH is an important coenzyme involved in more than 300 kinds of dehydrogenase enzymatic reactions. However, the electrochemical oxidation of NADH at a bare electrode in a neutral solution proceeds at a high oxidation potential (ca. +0.5 V) because of slow electron transfer kinetics and electrode fouling.[43] Thus, oxidation of NADH at a low potential is highly desirable for the development of NADH-based bioelectrochemical devices. Although the use of redox-active dyes such as MG offers an effective approach to the electrocatalytic oxidation of NADH, the stable confinement of these water-soluble molecules on substrate electrode remains technically difficult.[44] As demonstrated above, the MG-encapsulated SIM prepared here could not only be stably confined onto the electrode surface, but also will maintain the electrochemical properties of MG. These properties well enable the application of the SIM for the electrochemical sensing of NADH. As depicted in Figure 7C, the MG-encapsulated SIM-modified electrode shows a well-defined current response toward the successive addition of NADH into the buffer with a linear range from 20 to 160 μM at a low potential of −0.07 V.

This result demonstrates that the MG-encapsulated SIM shows good electrocatalytic activity for NADH oxidation and could thus be used for NADH sensing. As mentioned above, since NADH is an important coenzyme involved in more than 300 kinds of dehydrogenase enzymatic reactions, the SIM prepared in this study could be further used as a platform for the development of various kinds of dehydrogenase-based electrochemical biosensors and biofuel cells by combining with different kinds of dehydrogenases.

CONCLUSION

In summary, a new kind of SIM has been prepared by self-assembling imidazolium-based dication $C_{10}(mim)_2$ and ABTS dianion in water. The SIM shows good thermo-, water-, and salt-stability and excellent electrochemical/optical properties. Moreover, it shows adaptive encapsulation property toward heterocyclic dye molecules during the self-assembly process. Although some supramolecular ionic materials based on ionic self-assembly have been reported, the SIM demonstrated here with good water-stability and adaptive encapsulation properties remains unprecedented. This study introduces a new way to prepare water-stable and adaptive materials based on ionic interaction, which are particularly useful in many research fields such as biosensing, drug delivery, solid electrolyte, and ionic devices.

ASSOCIATED CONTENT

Supporting Information

Stoichiometry, salt stability, and adaptive encapsulation property of the SIM; confocal fluorescence images of AO-encapsulated SIM; and FT-IR to characterize the interaction between the dyes and ABTS. This material is available free of charge via the Internet at http://pubs.acs.org.

AUTHOR INFORMATION

Corresponding Authors

*E-mail: yuping@iccas.ac.cn. Fax: (+86)-10-6255-9373.
*E-mail: lqmao@iccas.ac.cn Fax: (+86)-10-6255-9373.

Notes

The authors declare no competing financial interest.

■ ACKNOWLEDGMENTS

This work is financially supported by NSF of China (Grant No. 21321003, 21127901, 21210007, and 91213305 for L. Mao; 91132708 and 21322503 for P. Yu), National Basic Research Program of China (973 Program, 2010CB933502), and the "Strategic Priority Research Program" of the Chinese Academy of Sciences (Grant No. XDA09020100).

■ REFERENCES

(1) Rybtchinski, B. Adaptive Supramolecular Nanomaterials Based on Strong Noncovalent Interactions. *ACS Nano* **2011**, *5*, 6791−6818.
(2) González-Rodríguez, D.; Schenning, A. P. H. J. Hydrogen-Bonded Supramolecular π-Functional Materials. *Chem. Mater.* **2010**, *23*, 310−325.
(3) Sanchez, C.; Boissiere, C.; Cassaignon, S.; Chaneac, C.; Durupthy, O.; Faustini, M.; Grosso, D.; Laberty-Robert, C.; Nicole, L.; Portehault, D.; Ribot, F.; Rozes, L.; Sassoye, C. Molecular Engineering of Functional Inorganic and Hybrid Materials. *Chem. Mater.* **2014**, *26*, 221−238.
(4) Ajayaghosh, A.; George, S. J. First Phenylenevinylene Based Organogels: Self-Assembled Nanostructures via Cooperative Hydrogen Bonding and π-Stacking. *J. Am. Chem. Soc.* **2001**, *123*, 5148−5149.
(5) Yamamoto, Y.; Fukushima, T.; Jin, W.; Kosaka, A.; Hara, T.; Nakamura, T.; Saeki, A.; Seki, S.; Tagawa, S.; Aida, T. A Glass Hook Allows Fishing of Hexa-peri-hexabenzocoronene Graphitic Nanotubes: Fabrication of a Macroscopic Fiber with Anisotropic Electrical Conduction. *Adv. Mater.* **2006**, *18*, 1297−1300.
(6) Babu, S. S.; Prasanthkumar, S.; Ajayaghosh, A. Self-Assembled Gelators for Organic Electronics. *Angew. Chem., Int. Ed.* **2012**, *51*, 1766−1776.
(7) Miyake, G. M.; Weitekamp, R. A.; Piunova, V. A.; Grubbs, R. H. Synthesis of Isocyanate-Based Brush Block Copolymers and Their Rapid Self-Assembly to Infrared-Reflecting Photonic Crystals. *J. Am. Chem. Soc.* **2012**, *134*, 14249−14254.
(8) Zhu, J.; Wang, J.; Lv, F.; Xiao, S.; Nuckolls, C.; Li, H. Synthesis and Self-Assembly of Photonic Materials from Nanocrystalline Titania Sheets. *J. Am. Chem. Soc.* **2013**, *135*, 4719−4721.
(9) Schenning, A. P. H. J.; Herrikhuyzen, J. V.; Jonkheijm, P.; Chen, Z.; Würthner, F.; Meijer, E. W. Photoinduced Electron Transfer in Hydrogen-Bonded Oligo(p-phenylene vinylene)−Perylene Bisimide Chiral Assemblies. *J. Am. Chem. Soc.* **2002**, *124*, 10252−10253.
(10) Yamamoto, Y.; Fukushima, T.; Suna, Y.; Ishii, N.; Saeki, A.; Seki, S.; Tagawa, S.; Taniguchi, M.; Kawai, T.; Aida, T. Photoconductive Coaxial Nanotubes of Molecularly Connected Electron Donor and Acceptor Layers. *Science* **2006**, *314*, 1761−1764.
(11) Delbosc, N.; Reynes, M.; Dautel, O. J.; Wantz, G.; Lère-Porte, J. P.; Moreau, J. J. E. Control of the Aggregation of a Phenylenevinylenediimide Chromophore by Use of Supramolecular Chemistry: Enhanced Electroluminescence in Supramolecular Organic Devices. *Chem. Mater.* **2010**, *22*, 5258−5270.
(12) Wang, M.; Lan, W.; Zheng, Y.; Cook, T. R.; White, H. S.; Stang, P. J. Post-Self-Assembly Covalent Chemistry of Discrete Multicomponent Metallosupramolecular Hexagonal Prisms. *J. Am. Chem. Soc.* **2011**, *133*, 10752−10755.
(13) Ortiz, M.; Fragoso, A.; O'Sullivan, C. K. Detection of Antigliadin Autoantibodies in Celiac Patient Samples Using a Cyclodextrin-Based Supramolecular Biosensor. *Anal. Chem.* **2011**, *83*, 2931−2938.
(14) Weis, M.; Waloch, C.; Seiche, W.; Breit, B. Self-Assembly of Bidentate Ligands for Combinatorial Homogeneous Catalysis: Asymmetric Rhodium-Catalyzed Hydrogenation. *J. Am. Chem. Soc.* **2006**, *128*, 4188−4189.
(15) Hu, J.; Guo, Y.; Liang, H.; Wan, L.; Jiang, L. Three-Dimensional Self-Organization of Supramolecular Self-Assembled Porphyrin Hollow Hexagonal Nanoprisms. *J. Am. Chem. Soc.* **2005**, *127*, 17090−17095.
(16) Nishiyabu, R.; Hashimoto, N.; Cho, T.; Watanabe, K.; Yasunaga, T.; Endo, A.; Kaneko, K.; Niidome, T.; Murata, M.; Adachi, C.; Katayama, Y.; Hashizume, M.; Kimizuka, N. Nanoparticles of Adaptive Supramolecular Networks Self-Assembled from Nucleotides and Lanthanide Ions. *J. Am. Chem. Soc.* **2009**, *131*, 2151−2158.
(17) Nishiyabu, R.; Aimé, C.; Gondo, R.; Kaneko, K.; Kimizuka, N. Selective Inclusion of Anionic Quantum Dots in Coordination Network Shells of Nucleotides and Lanthanide Ions. *Chem. Commun.* **2010**, *46*, 4333−4335.
(18) Nishiyabu, R.; Aimé, C.; Gondo, R.; Noguchi, T.; Kimizuka, N. Confining Molecules within Aqueous Coordination Nanoparticles by Adaptive Molecular Self-Assembly. *Angew. Chem., Int. Ed.* **2009**, *48*, 9465−9468.
(19) Huang, P.; Mao, J.; Yang, L.; Yu, P.; Mao, L. Bioelectrochemically Active Infinite Coordination Polymer Nanoparticles: One-Pot Synthesis and Biosensing Property. *Chem.—Eur. J.* **2011**, *17*, 11390−11393.
(20) Decher, G. Fuzzy Nanoassemblies: Toward Layered Polymeric Multicomposites. *Science* **1997**, *277*, 1232−1237.
(21) Faul, C. F. J.; Antonietti, M. Ionic Self-Assembly: Facile Synthesis of Supramolecular Materials. *Adv. Mater.* **2003**, *15*, 673−683.
(22) Zakrevskyy, Y.; Stumpe, J.; Faul, C. F. J. A Supramolecular Approach to Optically Anisotropic Materials: Photosensitive Ionic Self-Assembly Complexes. *Adv. Mater.* **2006**, *18*, 2133−2136.
(23) Huang, Y.; Yan, Y.; Smarsly, B. M.; Wei, Z.; Faul, C. F. J. Helical Supramolecular Aggregates, Mesoscopic Organisation and Nanofibers of a Perylenebisimide-Chiral Surfactant Complex via Ionic Self-Assembly. *J. Mater. Chem.* **2009**, *19*, 2356−2362.
(24) Wathier, M.; Grinstaff, M. W. Synthesis and Properties of Supramolecular Ionic Networks. *J. Am. Chem. Soc.* **2008**, *130*, 9648−9649.
(25) Guan, Y.; Yu, S.; Antonietti, M.; Böttcher, C.; Faul, C. F. J. Synthesis of Supramolecular Polymers by Ionic Self-Assembly of Oppositely Charged Dyes. *Chem.—Eur. J.* **2005**, *11*, 1305−1311.
(26) Anderson, J. L.; Ding, R.; Ellem, A.; Armstrong, W. Structure and Properties of High Stability Geminal Dicationic Ionic Liquids. *J. Am. Chem. Soc.* **2005**, *127*, 593−604.
(27) Zheng, W.; Li, Q.; Su, L.; Yan, Y.; Zhang, J.; Mao, L. Direct Electrochemistry of Multi-Copper Oxidases at Carbon Nanotubes Noncovalently Functionalized with Cellulose Derivatives. *Electroanalysis* **2006**, *18*, 587−594.
(28) Zebda, A.; Gondran, C.; Cinquin, P.; Cosnier, S. Glucose Biofuel Cell Construction based on Enzyme, Graphite Particle and Redox Mediator Compression. *Sens. Actuators, B* **2012**, *173*, 760−764.
(29) Shi, J.; Wu, P.; Yan, F. Further Investigation of the Intermolecular Interactions and Component Distributions in a $[Bmim][BF_4]^-$based Polystyrene Composite Membranes using Two-Dimensional Correlation Infrared Spectroscopy. *Langmuir* **2010**, *26*, 11427−11434.
(30) Zhuang, X.; Wang, D.; Lin, Y.; Yang, L.; Yu, P.; Jiang, W.; Mao, L. Strong Interaction between Imidazolium-Based Polycationic Polymer and Ferricyanide: Toward Redox Potential Regulation for Selective In Vivo Electrochemical Measurements. *Anal. Chem.* **2012**, *84*, 1900−1906.
(31) Zhou, Y.; Schattka, J. H.; Antonietti, M. Room-Temperature Ionic Liquids as Template to Monolithic Mesoporous Silica with Wormlike Pores via a Sol-Gel Nanocasting Technique. *Nano Lett.* **2004**, *4*, 477−481.
(32) Billard, I.; Moutiers, G.; Labet, A.; El Azzi, A.; Gaillard, C.; Mariet, C.; Lützenkirchen, K. Stability of Divalent Europium in an Ionic Liquid: Spectroscopic Investigations in 1-Methyl-3-butylimidazolium Hexafluorophosphate. *Inorg. Chem.* **2003**, *42*, 1726−1733.
(33) Paul, A.; Mandal, P. K.; Samanta, A. How Transparent are the Imidazolium Ionic Liquids? A Case Study with 1-Methyl-3-butylimidazolium Hexafluorophosphate. *Chem. Phys. Lett.* **2005**, *402*, 375−379.
(34) Mandal, P. K.; Paul, A.; Samanta, A. Excitation Wavelength Dependent Fluorescence Behavior of the Room Temperature Ionic

Liquids and Dissolved Dipolar Solutes. *J. Photochem. Photobiol., A* **2006**, *182*, 113−120.
(35) Paul, A.; Mandal, P. K.; Samanta, A. On the Optical Properties of the Imidazolium Ionic Liquids. *J. Phys. Chem. B* **2005**, *109*, 9148−9153.
(36) Bourbonnais, R.; Leech, D.; Paice, M. G. Electrochemical Analysis of the Interactions of Laccase Mediators with Lignin Model Compounds. *Biochim. Biophys. Acta, Gen. Subj.* **1998**, *1379*, 381−390.
(37) Liu, B.; Wen, L.; Nakata, K.; Zhao, X.; Liu, S.; Ochiai, T.; Murakami, T.; Fujishima, A. Polymeric Adsorption of Methylene Blue in TiO_2 Colloids: Highly Sensitive Thermochromism and Selective Photocatalysis. *Chem.—Eur. J.* **2012**, *18*, 12705−12711.
(38) McHedlov-Petrosyan, N. O.; Fedorov, L. A.; Sokolovskii, S. A.; Surov, Y. N.; Maiorga, R. S. Structural Conversions of Rhodamines in Solution. *Russ. Chem. Bull.* **1992**, *41*, 403−409.
(39) Zimmerman, F.; Hossenfelder, B.; Panitz, J. C.; Wokaun, A. SERRS study of Acridine Orange and Its Binding to DNA Strands. *J. Phys. Chem.* **1994**, *98*, 12796−12804.
(40) Kahr, B.; Gurney, R. W. Dyeing Crystals. *Chem. Rev.* **2001**, *101*, 893−952.
(41) Sours, R. E.; Fink, D. A.; Swift, J. A. Dyeing Uric Acid Crystals with Methylene Blue. *J. Am. Chem. Soc.* **2002**, *124*, 8630−8636.
(42) Lin, Y.; Zhu, N.; Yu, P.; Su, L.; Mao, L. Physiologically Relevant Online Electrochemical Method for Continuous and Simultaneous Monitoring of Striatum Glucose and Lactate Following Global Cerebral Ischemia/Reperfusion. *Anal. Chem.* **2009**, *81*, 2067−2074.
(43) Raj, C. R.; Ohsaka, T. Electrocatalytic Sensing NADH at an In Situ Functionalized Self-assembled Monolayer on Gold Electrode. *Electrochem. Commun.* **2001**, *3*, 633−638.
(44) Yan, Y.; Zhang, M.; Gong, K.; Su, L.; Guo, Z.; Mao, L. Adsorption of Methylene Blue Dye onto Carbon Nanotubes: A Route to an Electrochemically Functional Nanostructure and Its Layer-by-Layer Assembled Nanocomposite. *Chem. Mater.* **2005**, *17*, 3457−3463.